Mathematical Medicine and Biology: A Journal of the IMA (2019) **36**, 297–324
doi:10.1093/imammb/dqy011
Advance Access publication on 27 July 2018

Optimal public health intervention in a behavioural vaccination model: the interplay between seasonality, behaviour and latency period

Bruno Buonomo
Department of Mathematics and Applications, University of Naples Federico II, via Cintia, 80126 Naples, Italy

Rossella Della Marca
Department of Mathematical, Physical and Computer Sciences, University of Parma, Parco Area delle Scienze 53/A, 43124 Parma, Italy

and

Alberto d'Onofrio*
International Prevention Research Institute, 95 Cours Lafayette, 69006 Lyon, France
*Corresponding author. Email: alberto.donofrio@i-pri.org

[Received on 21 December 2017; revised on 2 July 2018; accepted on 3 July 2018]

Hesitancy and refusal of vaccines preventing childhood diseases are spreading due to 'pseudo-rational' behaviours: parents overweigh real and imaginary side effects of vaccines. Nonetheless, the 'Public Health System' (PHS) may enact public campaigns to favour vaccine uptake. To determine the optimal time profiles for such campaigns, we apply the optimal control theory to an extension of the susceptible-infectious-removed (SIR)-based behavioural vaccination model by d'Onofrio *et al*. (2012, *PLoS ONE*, 7, e45653). The new model is of susceptible-exposed-infectious-removed (SEIR) type under seasonal fluctuations of the transmission rate. Our objective is to minimize the total costs of the disease: the disease burden, the vaccination costs and a less usual cost: the economic burden to enact the PHS campaigns. We apply the Pontryagin minimum principle and numerically explore the impact of seasonality, human behaviour and latency rate on the control and spread of the target disease. We focus on two noteworthy case studies: the low (resp. intermediate) relative perceived risk of vaccine side effects and relatively low (resp. very low) speed of imitation. One general result is that seasonality may produce a remarkable impact on PHS campaigns aimed at controlling, via an increase of the vaccination uptake, the spread of a target infectious disease. In particular, a higher amplitude of the seasonal variation produces a higher effort and this, in turn, beneficially impacts the induced vaccine uptake since the larger is the strength of seasonality, the longer the vaccine propensity remains large. However, such increased effort is not able to fully compensate the action of seasonality on the prevalence.

Keywords: vaccination; behaviour; vaccine hesitancy; behavioural epidemiology; optimal control; game theory; seasonality; latency; SEIR; imitation game; public health.

1. Introduction

Childhood infectious diseases are one of the main threats to children health. In 2016 measles alone caused 89,780 deaths, mainly among children under the age of 5, and many more serious sequelae (World Health Organization, 2017). Vaccination is one of the most effective methods to reduce the morbidity and mortality from vaccine-preventable infectious diseases (Andre *et al.*, 2008; Centers for Disease Control and Prevention, 2017). Although very effective in preventing the target diseases, due to

a number of cultural, social and political factors, many vaccines are often no more mandatory but voluntary and a trend towards the decrease of the adherence to vaccination campaigns for some vaccines (e.g. seasonal flu and measles-mumps-rubella (MMR) vaccines) has been frequently observed in many countries (Jansen *et al.*, 2003; Casiday *et al.*, 2006; Omer *et al.*, 2009; Dubé *et al.*, 2013).

This important wave of vaccine hesitancy and refusal caused the widespread resurgence of some vaccine-preventable diseases that were previously close to elimination thanks to the introduction of vaccinations (Jansen *et al.*, 2003). Emblematic are the recent measures adopted by the Italian and French governments to contrast vaccine hesitancy (Istituto Superiore di Sanità, 2017; Ministère des Solidarités et de la Santé, 2017). The abovementioned reduction of vaccine uptake is due to the spread of 'pseudo-rational' behaviours where parents overweigh the (real and imaginary) risk of vaccine side effects (VSEs) and do not fully perceive the actual risks linked to the disease (d'Onofrio *et al.*, 2008; Manfredi & d'Onofrio, 2013). This is paradoxically due to the vaccine-induced rarity of the disease. In fact, due to the rarity of the disease, many hesitant parents ask themselves the following question (which may seem rational): 'Since the disease X is eliminated/very rare in my country, why should we expose our babies to the VSEs?' Of course this reasoning does not take into account that the disease is eliminated/rare because of the large levels of vaccine uptake! Moreover, other parents, slightly more aware of the disease-related risks, adopt 'vaccination free riding': they avoid the perceived VSEs for their children by relying on herd immunity effects (Metcalf *et al.*, 2015; Sobo, 2016). This second type of behaviour does not take into the account that herd immunity is not static and permanent but it is dynamically evolving and, of course, it strongly depends on the widespread adherence to vaccination campaigns. Mathematically, similar classes of behaviours have been inferred by applying Mean Fields Games in Laguzet & Turinici (2015) and Salvarani & Turinici (2018) for time-continuous and time-discrete models without vital dynamics and with adult voluntary vaccinations.

Nonetheless, the 'Public Health System' (PHS) may enact public campaigns to favour vaccine uptake.

Given the increasing relevance of the abovementioned phenomena, classical models of mathematical epidemiology cannot be universally applied and a new discipline has arisen in the past 10 years: the 'behavioural epidemiology of infectious diseases' (BEID) (Manfredi & d'Onofrio, 2013; Wang *et al.*, 2016). The BEID aims at integrating in models of the spread and control of infectious diseases the role played by human behaviours and misbehaviours (Manfredi & d'Onofrio, 2013; Wang *et al.*, 2016). We shortly mention that behaviour has also a deep impact in modulating the transmission of infectious diseases, as first modelled in the seminal 1978 paper by Capasso & Serio (1978).

Game-theoretic analysis has been widely used in BEID, especially to model vaccine decision-making by examining individuals' pay-offs based on the perceived benefits and risks of vaccination (e.g. Bauch, 2005; Perisic & Bauch, 2009; Shim *et al.*, 2009; d'Onofrio *et al.*, 2011, Fu *et al.*, 2011; Reluga & Galvani, 2011; d'Onofrio *et al.*, 2012; Mbah *et al.*, 2012; Buonomo *et al.*, 2018a, n.d.). A classical game-theoretic model of personal choices is the 'imitation game' (Bauch, 2005; d'Onofrio *et al.*, 2011; Fu *et al.*, 2011; d'Onofrio *et al.*, 2012; Mbah *et al.*, 2012; Buonomo *et al.*, 2018a, n.d.). The basic idea is that parents' decision to vaccinate or to not vaccinate their children is conducted by imitating others who appear to have adopted more successful strategies. This occurs through the channels of the spontaneous 'private' communication. For example, such approach was adopted in Bauch (2005) (coupled with a SIR model), under the assumption that the perceived risk of suffering significant morbidity upon infection is a function of the prevalence of the disease and that the perceived risk of vaccination is constant. The authors of d'Onofrio *et al.* (2011) went a step beyond by adding the hypothesis that the exchange of group from 'vaccinators' to 'nonvaccinators' is not constant but depending on the available information and/or rumours on VSEs.

In d'Onofrio *et al.* (2012) the same authors of d'Onofrio *et al.* (2011) modified their imitation game model, taking into account the abovementioned public campaigns (including information, education, availability of vaccination infrastructures, etc.) of the PHS aimed at increasing vaccine uptake. Under these assumptions, the model predicts that public health interventions (PHIs) have a stabilizing role which may eliminate the disease and, in any case, reduce the strength of imitation-induced oscillations. This is a rather realistic scenario, since it depicts the widely observed large (although most often not enough) propensity to vaccinate children. For example, in England and Wales public campaigns allowed to achieve a large MMR vaccine uptake (Public Health Wales Protection Division, 2013, 2017; Screening, 2016), although under the elimination threshold.

In d'Onofrio *et al.* (2012) the efforts provided by PHS to increase the propensity to vaccinate are represented by a constant term. This is an acceptable approximation provided that the economic resources largely overcome the costs of enacting the awareness campaign. However, due to the presence of limited resources, it is desirable for public systems to jointly minimize disease-related social and economic costs.

A classical tool to predict the impact of optimal prevention and treatment efforts on infectious diseases is optimal control theory (OCT) (Fleming & Rishel, 1975; Arnautu *et al.*, 1989; Lenhart & Workman, 2007; Grass *et al.*, 2008; Anita *et al.*, 2011; Ledzewicz & Schättler, 2011; Ndeffo Mbah & Gilligan, 2013; Mwanga *et al.*, 2015; Ledzewicz *et al.*, 2016; Gromov *et al.*, 2017; Sharomi & Malik, 2017).

In Buonomo *et al.* (n.d.) OCT has been applied to the model introduced in d'Onofrio *et al.* (2012) to determine a suitable PHS effort that minimizes economic costs under given constraints in a given time horizon.

A strong limitation to the applicability of the behavioural model in study is that it is built on top of the well-known classical SIR compartmental epidemic model. However, SIR models do not consider the latency time occurring between the contagion and the onset of infectivity, i.e. needed for the viral population to pass from a relatively small population size to a size sufficiently large to potentially cause the contagion of a susceptible subject. On the contrary, this time interval in some childhood infectious diseases may be significant (NSW Ministry of Health, 2014). Its inclusion leads to the well-known SEIR epidemic model (Capasso, 1993; Earn *et al.*, 2000; d'Onofrio, 2002; Sun & Hsieh, 2010; De la Sen *et al.*, 2012; Buonomo *et al.*, 2013).

Moreover, the time series of diseases such as measles, chickenpox and mumps (all characterized by appreciable latency time) can exhibit both periodical and more complex patterns that are apparently fully erratic. This variety of patterns has been successfully explained by means of SEIR models with periodic contact rates undergoing non-linear resonances phenomena (including chaos) (Altizer *et al.*, 2006; Grassly & Fraser, 2006; Buonomo *et al.*, 2018b). The key idea is that the transmission strongly depends on school calendar with its yearly alternation of school terms, characterized by a large number of contacts at risk, and holidays, with a smaller number of contacts at risk. Moreover, such alternation can also impact on the stability of disease-free states. As far as the behavioural issues are concerned, in Buonomo *et al.* (2018a) it has been shown that the fluctuating contact rate has important effects also on PHS intervention-induced disease elimination, provided that the disease has a latency time.

These results of classical and behavioural epidemiology suggest that a periodically varying transmission rate could impact on the disease spread under optimal control of the vaccine awareness campaigns and on the time profile of the control. The investigation of this problem, which is the aim of our work, has to take into account the multiple interlinked factors determining the system's dynamics: i) the optimal temporal efforts of PHS in affecting perceptions about the disease and vaccines with

minimum costs; ii) the yearly periodic fluctuations of the transmission rate, which act as a periodic forcing on a system that is both non-linear and under optimal control; iii) the possible effect of the latency time that is the most specific biological parameter of the SEIR model; and finally iv) populations with identical demographic and biological features can exhibit different behavioural responses.

Namely, we will consider two behavioural scenarios. In the first scenario, we assume that the population perceives a relatively low relative risk of VSEs, and that its imitation speed is relatively low. In the second scenario the perceived relative risk of VSEs is larger, and the imitation speed is very low.

The paper is organized as follows. In Section 2 the model is introduced. In Section 3 the optimal control (OC) problem is formulated and parametrized. In Section 4 the demographic and epidemiological parameter values are discussed. Then, in the next two sections, the numerical simulations are presented for the two above-illustrated behavioural scenarios. The impact of the latency rate on the dynamics and the control of the model is discussed in Section 7. Concluding remarks follow in Section 8. This work ends with a short appendix on the possible impact of demographic trends.

2. The model

2.1 *Model formulation*

We consider an infectious childhood disease controlled by a 100% effective vaccine ensuring lifelong immunity. Its time evolution is ruled by the following information-dependent SEIR model:

$$\begin{aligned} \dot{S} &= \mu(1-p) - \mu S - \beta(t)SI \\ \dot{E} &= \beta(t)SI - (\mu+\rho)\,E \\ \dot{I} &= \rho E - (\mu+\nu)\,I \\ \dot{R} &= \nu I - \mu R, \end{aligned} \tag{2.1}$$

where S, E, I and R are functions of time denoting the fractions of susceptible, latent, infectious and removed individuals at time t, respectively. The upper dot denotes the time derivative. A fifth compartment, the fraction of vaccinated individuals, V, can be derived as

$$V = 1 - S - E - I - R.$$

Vaccination is administered at birth alone and the uptake level is time-dependent; hence, p represents the 'propensity to vaccinate' among parents at time t (Bauch, 2005; d'Onofrio *et al.*, 2011, 2012; Buonomo *et al.*, 2018a, n.d.). The parameters are positive constants: μ is the natural death rate, which is assumed to be identical to the birth rate; ρ is the inverse of the latency period and ν is the inverse of the average length of the infectious period. In order to account the effects of seasonal variations on the disease transmission, the transmission rate $\beta(t)$ is modelled as a sinusoidal function

$$\beta(t) = \beta_{avg}\left[1 + \sigma\cos\left(\omega t + \chi\right)\right], \tag{2.2}$$

where β_{avg} is the average transmission rate, σ is the amplitude of the seasonal variation, with $0 \leqslant \sigma < 1$, ω is the pulsation and χ is the phase.

As far as p is concerned, we assume that the population of parents is proportional to the total (constant) population N and is divided into two subgroups. The first subgroup is given by parents who

are pro-vaccine and vaccinate their children (p); the second one is given by parents who are hesitant or overtly against vaccination and, as a consequence, do not vaccinate their children ($A = 1 - p$).

The 'imitation' game is a 'mutual contagion of ideas' process (Wang *et al.*, 2016)

$$\dot{p} = -F_A(A,p)p + F_P(A,p)A$$
$$\dot{A} = F_A(A,p)p - F_P(A,p)A,$$

where $F_A(A,p)$ and $F_P(A,p)$ are the 'forces of infection' of the opinions of the anti-vaccination and pro-vaccination group, respectively. We assume the following:

$$F_A(A,p) = \alpha^* A, \quad F_P(A,p) = \theta^* p,$$

where α^* and θ^* are the transmission rates of the group p and A, respectively. Following Buonomo *et al.* (2018a), Buonomo *et al.* (n.d.) and d'Onofrio *et al.* (2012), we further assume that α^* depends on the current information on VSEs, i.e. $\alpha^* = \alpha(p)$, and θ^* depends on the perceived risk of being infected and/or suffering serious consequences from the disease, i.e. $\theta^* = \theta(I)$. In general both functions $\alpha(p)$ and $\theta(I)$ are assumed to be increasing and positive, although we limit ourselves to consider the linear case

$$\alpha(p) = k_0 \alpha p, \qquad \theta(I) = k_0 \theta I,$$

where α, θ and the scale factor k_0 are positive constants.

The PHIs in favour of vaccination propensity can be modelled as an additional transfer rate from A to p yielding

$$\begin{aligned} \dot{p} &= -k_0 \alpha A p^2 + k_0 \theta I p A + \gamma(t) A \\ \dot{A} &= k_0 \alpha A p^2 - k_0 \theta I p A - \gamma(t) A, \end{aligned} \tag{2.3}$$

where $\gamma(t)$ is a positive function, which represents the effectiveness of a public campaign (information, education, availability of vaccination infrastructures, etc.) in affecting individuals' perceptions about both the infection and VSEs. We assume that the induced flux is linearly proportional to the fraction of parents that are opposed to vaccination.

Since $A = 1 - p$, from (2.3) one gets the following extension of an imitation game equation:

$$\dot{p} = (1-p)\left[\left(k_0 \theta I - k_0 \alpha p\right) p + \gamma(t)\right]. \tag{2.4}$$

Coupling (2.4) to the epidemic model (2.1) and (2.2) we obtain a non-linear, non-autonomous ordinary differential equation (ODE) system (say, SEIRp model)

$$\begin{aligned} \dot{S} &= \mu(1-p) - \mu S - \beta_{avg}\left[1 + \sigma\cos(\omega t + \chi)\right] SI \\ \dot{E} &= \beta_{avg}\left[1 + \sigma\cos(\omega t + \chi)\right] SI - (\mu + \rho) E \\ \dot{I} &= \rho E - (\mu + \nu) I \\ \dot{R} &= \nu I - \mu R \\ \dot{p} &= (1-p)\left[\left(k_0 \theta I - k_0 \alpha p\right) p + \gamma(t)\right]. \end{aligned} \tag{2.5}$$

The following initial conditions are assumed to be non-negative:

$$S(0) = S_0 \geqslant 0,\ E(0) = E_0 \geqslant 0,\ I(0) = I_0 \geqslant 0,\ R(0) = R_0 \geqslant 0,\ p(0) = p_0 \geqslant 0. \tag{2.6}$$

2.2 *Basic properties*

It is easy to check that the set

$$\mathfrak{D} = \left\{(S, E, I, R, p) \in \mathbb{R}^5_+ : S + E + I + R \leqslant 1,\ p \leqslant 1\right\}$$

is positively invariant, i.e. solutions of (2.5) with initial conditions in $\mathfrak{D}$ remain in $\mathfrak{D}$ for all $t \geqslant 0$. Therefore, the investigation may be limited to this region.

For reference purposes, let us consider model (2.5) in the case of constant control, i.e. $\gamma(t) = \widetilde{\gamma}(const.)$. In this case the model admits two disease-free equilibria: the pure vaccinator equilibrium (PVE) given by

$$E_1 = (0, 0, 0, 0, 1),$$

and the mixed-state equilibrium (MSE) given by

$$E_2 = \left(1 - \sqrt{\frac{\widetilde{\gamma}}{k_0\alpha}}, 0, 0, 0, \sqrt{\frac{\widetilde{\gamma}}{k_0\alpha}}\right),$$

which exists (i.e. it is positive) only if $\widetilde{\gamma} < k_0\alpha$.

It can be proved that the following theorem holds (see Buonomo *et al.*, 2018a for the proof):

THEOREM 2.1 If $\widetilde{\gamma} \geqslant k_0\alpha$, then the PVE is the only equilibrium of model (2.5) and is globally asymptotically stable (GAS) in $\mathfrak{D}$; if $\widetilde{\gamma} < k_0\alpha$, then the PVE is unstable and there exists also the MSE equilibrium. Furthermore, there exist two threshold values, $\widetilde{\gamma}_{cr}$ and $\widetilde{\gamma}_*$, where $\widetilde{\gamma}_{cr} < \widetilde{\gamma}_*$ and $\widetilde{\gamma}_{cr}$ depends on the amplitude σ, such that

- if $\widetilde{\gamma}_* < \widetilde{\gamma} < k_0\alpha$, then the MSE is GAS, independent from the oscillations of the transmission rate;
- if $\widetilde{\gamma}_{cr}(\sigma) < \widetilde{\gamma} < \widetilde{\gamma}_*$, then the MSE is GAS, and in this case the stability depends on σ;
- if $\widetilde{\gamma} < \widetilde{\gamma}_{cr}(\sigma)$, then the MSE is unstable and the disease is persistent.

3. The optimal control problem

In this section, we investigate the optimal time profile of PHIs aimed at increasing the propensity to vaccinate in a non-mandatory immunization regime. Our goal is to jointly minimize disease-related costs, vaccination (and VSEs) costs and enactment cost of the strategy. To this aim, the objective functional to be minimized includes the following three components (where a discount rate r is taken into account):

- 'Costs due to the disease burden.' The first cost component is the total direct and indirect (loss of productivity, social alarm, etc.) costs caused by all new infectious subjects during the time

horizon $[0, t_f]$ which reads

$$J_{in} = K_{in} \int_0^{t_f} e^{-rt} N \rho E \, \mathrm{d}t,$$

where K_{in} is the average cost for a new infectious case, and N denotes the total (constant) population. By setting the costs dependent on the incidence of the disease, we want to minimize the 'flux' of the new infectious, indirectly reducing the global burden. It is interesting to note that if $r = 0$ then from the second equation of system (2.1) it follows

$$J_{in} = \frac{K_{in} N \rho}{\mu + \rho} \left[E_0 - E(t_f) + \int_0^{t_f} \beta(t) SI \, \mathrm{d}t \right],$$

where the last addendum in parenthesis is the number of people that were infected in $[0, t_f]$.

- 'Costs of vaccination and VSEs.' Denoting with K_v the average cost of vaccine administration per person and potential costs deriving from VSEs, it follows that the global cost of vaccinations and VSEs is

$$J_v = K_v \int_0^{t_f} e^{-rt} N \mu p \, \mathrm{d}t.$$

- 'Public campaign costs'. In the lack of real data, we assume that Public Health (PH) efforts are increasingly costly, and that nonlinearity might mainly arise at high intervention levels. Therefore, we assume that the integrand function is quadratic with respect to the control variable $\gamma(t)$. This approach is widely employed in applications of OCT to mathematical epidemiology (Blayneh *et al.*, 2010; Lee *et al.*, 2010; Prosper *et al.*, 2014; Rodrigues *et al.*, 2014). Therefore, we have

$$J_\gamma = C_\gamma \int_0^{t_f} e^{-rt} \gamma^2(t) \, \mathrm{d}t,$$

where C_γ is a positive constant. In the present case, the quadratic cost can be qualitatively justified as follows (Buonomo *et al.*, n.d.): i) the cost per time unit is very likely an increasing function of the number of people that switch from the no-vaccine to the vaccine strategy, which is equal to $N\gamma(t)(1-p)$; ii) the cost per time unit is also an increasing function of the induced speed of strategy change $\gamma(t)$; iii) the cost per time unit ought to be a decreasing function of the hesitant/hostile population (fraction: $(1-p)$); iv) if very few anti-vaccinators remain, the cost to convince them is very large, say, it tends to plus infinity. Thus, in the easiest case, by assuming that the cost per time unit is proportional to both $\gamma(t)(1-p)$ and $\gamma(t)$ and inversely proportional to $1-p$ one gets a quadratic cost.

By setting $C_\varphi = K_{in} N \rho$ and $C_v = K_v N \mu$, our goal can be formalized as follows: 'find an optimal control function $\gamma^*(t)$ that minimizes the objective functional

$$J(\gamma(t)) = J_{in} + J_v + J_\gamma = \int_0^{t_f} e^{-rt} \left[C_\varphi E + C_v p + C_\gamma \gamma^2(t) \right] \mathrm{d}t \tag{3.1}$$

on the admissible set

$$\Omega = \left\{ \gamma(t) \in L^1\left(0, t_f\right), 0 \leqslant \gamma(t) \leqslant \gamma_{\max} \right\},$$

subject to (2.5) and initial conditions (2.6).'

The assumption of upper boundedness for $\gamma(t)$ reflects the realistic scenario of practical limitations on the maximum rate at which public information may spread during a given time interval.

The existence of the optimal control solution $\gamma^*(t)$ for this problem is guaranteed because the requirements of classical existence theorems (i.e. Theorem III.4.1 and its corresponding corollary in Fleming & Rishel, 1975) are satisfied.

Regarding its characterization, according to Pontryagin's minimum principle (Pontryagin *et al.*, 1962), the problem of finding the time-dependent control variable $\gamma^*(t)$ that minimizes the objective functional (3.1) is equivalent to the problem of minimizing the 'current value' Hamiltonian:

$$H = C_\varphi E + C_v p + C_\gamma \gamma^2(t) + \boldsymbol{\lambda} \cdot \mathbf{f}.$$

Here $\mathbf{f}$ denotes the right-hand side of (2.5) and $\boldsymbol{\lambda} \in \mathbb{R}^5$ the 'adjoint' variables vector at time t. The latter is the solution of the adjoint system

$$\dot{\boldsymbol{\lambda}} = r\boldsymbol{\lambda} - \frac{\partial H}{\partial \mathbf{x}},$$

with the 'transversality condition'

$$\boldsymbol{\lambda}\left(t_f\right) = \mathbf{0},$$

where $\mathbf{x}$ denotes the state variables vector.

In our case, the adjoint system is the following:

$$\begin{aligned}
\dot{\lambda_1} &= r\lambda_1 + \left(\lambda_1 - \lambda_2\right)\beta_{avg}\left[1 + \sigma\cos\left(\omega t + \chi\right)\right]I + \mu\lambda_1 \\
\dot{\lambda_2} &= r\lambda_2 - C_\varphi + \rho\left(\lambda_2 - \lambda_3\right) + \mu\lambda_2 \\
\dot{\lambda_3} &= r\lambda_3 + \left(\lambda_1 - \lambda_2\right)\beta_{avg}\left[1 + \sigma\cos\left(\omega t + \chi\right)\right]S + \lambda_3\left(\mu + \nu\right) - \nu\lambda_4 - k_0\theta\lambda_5\left(p - p^2\right) \\
\dot{\lambda_4} &= r\lambda_4 + \mu\lambda_4 \\
\dot{\lambda_5} &= r\lambda_5 - C_v + \mu\lambda_1 + \lambda_5\left[k_0\left(-3\alpha p^2 + 2\alpha p + 2\theta I p - \theta I\right) + \gamma(t)\right].
\end{aligned}$$

The optimal control $\gamma^*(t)$ that solves the control problem is the time-dependent function that minimizes H. In other words, it must satisfy the following:

$$\frac{\partial H}{\partial \gamma} = 0, \quad \text{and} \quad \frac{\partial^2 H}{\partial \gamma^2} > 0.$$

More explicitly, we have

$$\begin{aligned} H = {} & C_\varphi E + C_v p + C_\gamma \gamma^2(t) \\ & + \lambda_1 \left[\mu(1-p) - \mu S - \beta_{avg}\left[1 + \sigma\cos(\omega t + \chi)\right] SI\right] \\ & + \lambda_2 \left[\beta_{avg}\left[1 + \sigma\cos(\omega t + \chi)\right] SI - (\mu + \rho) E\right] \\ & + \lambda_3 \left[\rho E - (\mu + \nu) I\right] \\ & + \lambda_4 (\nu I - \mu R) \\ & + \lambda_5 \left[k_0 \left(\alpha p^3 - \alpha p^2 - \theta I p^2 + \theta I p\right) + \gamma(t) - p\gamma(t)\right]. \end{aligned} \tag{3.2}$$

Note that we have rewritten (2.4) as follows:

$$\dot{p} = k_0\left(\alpha p^3 - \alpha p^2 - \theta I p^2 + \theta I p\right) + \gamma(t) - p\gamma(t).$$

Differentiating H with respect to the control and solving for $\gamma(t)$, we obtain the following:

$$\gamma^*(t) = \min\left(\max\left(0, \frac{(p^* - 1)\lambda_5}{2C_\gamma}\right), \gamma_{\max}\right) \tag{3.3}$$

and

$$\frac{\partial^2 H}{\partial \gamma^2} = 2C_\gamma > 0.$$

The notation with superscript * is used to denote the solution to the state system (2.5) corresponding to the optimal control $\gamma^*(t)$.

4. Demographic and epidemiological parameter values

4.1 *Human behaviour and seasonality parameters*

We want to explore the impact of seasonality and human behaviour on the control of the spread of the target disease. First of all, for convenience, we introduce the quantities $\overline{\alpha} = \alpha/\theta$, and $\overline{k} = k_0\theta$, which can be interpreted, respectively, as the normalized measure of the relative perceived risk of VSEs compared to the perceived risk of infection and the normalized index of imitation or 'internal' influence (d'Onofrio *et al.*, 2012).

One of the main features of a behavioural epidemic model is constituted by the part modelling the dynamics of the time-changing vaccine propensity p, namely, in our case, the imitation game equation. As a consequence, in order to investigate the impact of the human behaviour on the optimal control and the disease spread, we consider the following two case studies:

- **CASE I**: $(\overline{\alpha}, \overline{k}) = (1/2000, 200)$, corresponding to a low perceived relative risk of VSEs and relatively slow imitation;
- **CASE II**: $(\overline{\alpha}, \overline{k}) = (1/450, 5)$, corresponding to an intermediate perceived relative risk of VSEs and very slow imitation.

TABLE 1 *Many demographic and epidemiological parameters and baseline values for model (2.5).*

Parameter	Description	Baseline value
μ	Birth/death rate (per day)	$1/(78 \times 365)$
β_{avg}	Average transmission rate (per day)	1.4294
ε	Immigration/emigration flux (per day)	2.2×10^{-6}
ρ	Latency rate (per day)	1/10
ν	Recovery rate (per day)	1/7
σ	Amplitude of the transmission rate	[0,1)
ω	Pulsation of the transmission rate (per day)	$2\pi/365$
χ	Phase of the transmission rate	-0.8
N	Total population	5×10^6
S_0	Initial fraction of susceptible individuals	0.055
E_0	Initial fraction of latent individuals	9×10^{-6}
I_0	Initial fraction of infectious individuals	8×10^{-6}
p_0	Initial vaccinated proportion among newborns	0.95

The large disproportion between α and θ is a consequence of the assumption that the perceived risk of infection is prevalence-dependent. Indeed, in d'Onofrio *et al.* (2011) it was shown that this is a necessary condition in order to achieve high coverages.

All the parameter values are described in Table 1. Data are based on previous studies (Buonomo *et al.*, 2018a, n.d.). In particular, choosing 1 day as time unit, it follows that the pulsation ω of the transmission rate (2.2) is $\omega = 2\pi/365$. The phase is assumed to be $\chi = -0.8$, in order to represent a maximum value in correspondence to school terms (February) and a minimum value for summer holidays (August). The amplitude range is $[0, 1)$ to preserve the positivity of the transmission rate.

As mentioned above, we are also interested in assessing the impact of seasonality on the control. At this aim, we explore three cases:

(a) low seasonality, represented by the case $\sigma = 0.2$;

(b) moderate seasonality, $\sigma = 0.5$;

(c) large seasonality, $\sigma = 0.9$,

complemented by the 'baseline case' of absence of seasonality: $\sigma = 0$.

4.2 *Numerical algorithms and parametrization of the optimal control problem*

We use the gradient descent or steepest descent method (Anita *et al.*, 2011) to investigate numerically the optimal control problem. The fourth-order Runge–Kutta method is used to perform all the numerical integrations.

As in Bauch (2005), we include a small immigration/emigration constant flux ε to take into the account of immigration of infected individuals during inter-epidemic periods. Precisely, in model (2.5) a positive influx $+\varepsilon$ is added to the second equation, balanced by a negative term $-\varepsilon$ in the first equation. Clearly, this constant influx term must be taken into account also in (3.2).

The temporal horizon is set $t_f = 11$ years, i.e. we focus on the medium term impact of the PHS efforts. Under the assumption of low inflation rate, we can safely disregard the discount rate (i.e. $r = 0$).

In order to emphasize the difficulties to increase the propensity to vaccinate, we set $\gamma_{\max}$ at a level below the threshold $k_0\alpha = \bar{k}\bar{\alpha}$ that would ensure global stability of the PVE in model (2.5) with constant $\gamma(t)$ and $\varepsilon = 0$. In particular, in our simulations we will use $\gamma_{\max} = 0.9\bar{k}\bar{\alpha}$.

As far as costs are concerned, following Carabin *et al.* (2002), we set $K_{in} = 307$, which corresponds to the average cost per measles case in UK. The unit cost of vaccination, K_v, is computed as the sum of two components: the cost of a single vaccine dose, 19 USD (for an MMR dose), and the average direct cost of an episode of VSEs, 2.08 USD.

As for C_γ, given the lack of real data, we roughly infer its order of magnitude by the following considerations. Let us consider the case of constant control $\gamma(t) = \widetilde{\gamma}(const.)$, with $0 < \widetilde{\gamma} < \bar{k}\bar{\alpha}$, and $\varepsilon = 0$. Evaluating the total cost for unit time at the MSE, we have

$$\bar{J}(\widetilde{\gamma}) = K_v N\mu\sqrt{\frac{\widetilde{\gamma}}{\bar{k}\bar{\alpha}}} + C_\gamma\widetilde{\gamma}^2.$$

In order to estimate C_γ, we may assume that, given a suitable value of $\widetilde{\gamma}$, the cost of enacting a public campaign has the same order of magnitude of the total costs arising from vaccination, i.e.

$$C_\gamma\widetilde{\gamma}^2 \approx K_v N\mu\sqrt{\frac{\widetilde{\gamma}}{\bar{k}\bar{\alpha}}},$$

or equivalently

$$C_\gamma \approx \frac{1}{\widetilde{\gamma}^2}K_v N\mu\sqrt{\frac{\widetilde{\gamma}}{\bar{k}\bar{\alpha}}} = \frac{K_v N\mu}{\widetilde{\gamma}\sqrt{\bar{k}\bar{\alpha}\widetilde{\gamma}}},$$

which provides a baseline approximation for C_γ. In our simulations we assume that $\widetilde{\gamma} = \gamma_{\max}$.

Parameter values of the optimal control problem are collected in Table 2.

As far as initial conditions are concerned, they revealed to be critical for the chosen algorithms. Indeed, we initially intended to employ for both Cases I and II the respective *endemic equilibrium* (say, EE) in the case of constant contact rate ($\beta(t) = \beta_{avg}$). However, we used two different methods, the gradient descent method (Anita *et al.*, 2011) and the forward–backward sweep method (Lenhart & Workman, 2007) but both of them failed to converge for numerical experiments we had designed. Thus,

TABLE 2 *Parameters and baseline values of the optimal control problem defined in Section 3.*

Parameter	Description	Baseline value
r	Discount rate (per day)	0
$\gamma_{\max}$	Maximum rate of PHS efforts (per day)	$0.9\bar{k}\bar{\alpha}$
K_{in}	Average unit cost per infectious case (USD)	307
K_v	Average unit cost of vaccination (USD)	21.08
C_γ	Cost of strategy implementation (USD)	$K_v N\mu/\left(\gamma_{\max}\sqrt{\bar{k}\bar{\alpha}\gamma_{\max}}\right)$
t_f	Length of the planning horizon (in days)	11×365

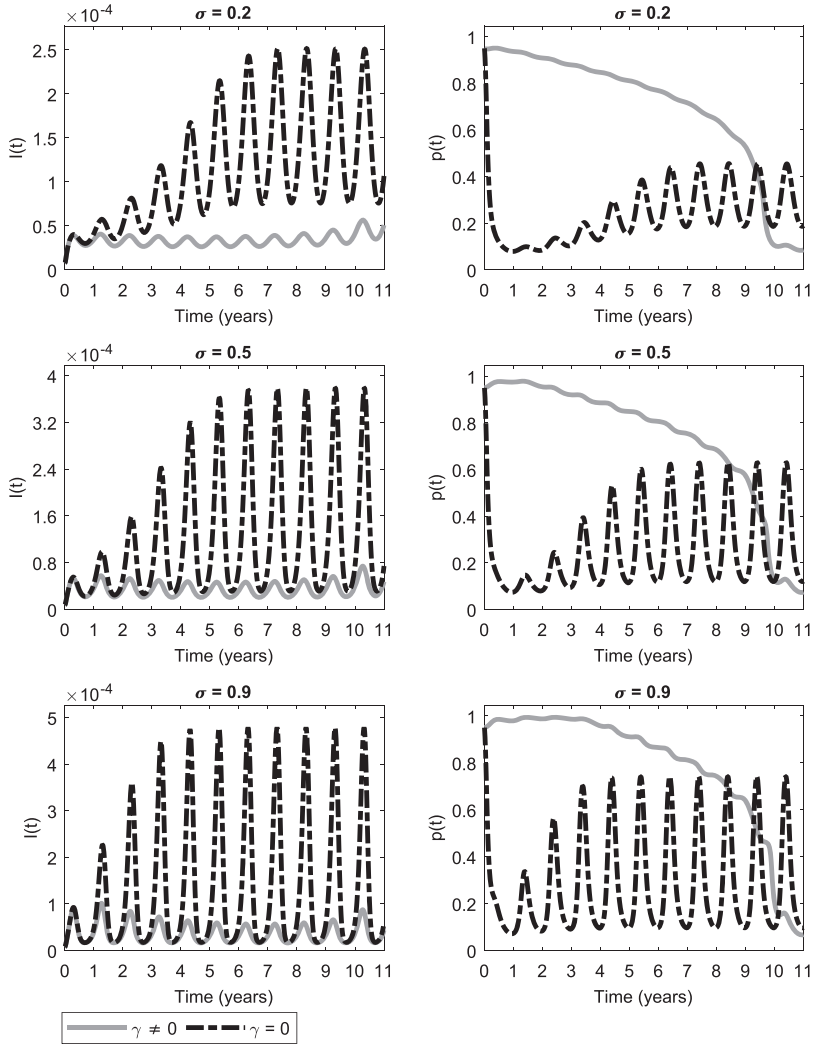

FIG. 1. Case I (low perceived relative risk of VSEs and relatively slow imitation): impact of the seasonality amplitude σ on the dynamics of model (2.5). The dash-dotted (resp. solid) lines represent the time profiles in absence of control ($\gamma(t) \equiv 0$) (resp. with the optimal control given by (3.3)). Left panels: fraction of infectious individuals. Right panels: vaccinated proportion among newborns. First row: $\sigma = 0.2$, second row: $\sigma = 0.5$ and third row: $\sigma = 0.9$. The other parameter values are reported in Tables 1 and 2.

the use of the above important initial conditions severely limited the full exploration of the effects of contact rate oscillations of human behaviour and of the latency time. As a consequence, we had to use a slightly different initial conditions adopted in Buonomo *et al.* (2018a), which are slight perturbations of EE. Furthermore, we assumed $p_0 = 0.95$. As far as the possible reasons of the lack of convergence are concerned, we stress that even in absence of the control the system is particularly stiff. To mitigate its stiffness we adopted some variable transformations that help and accelerate the simulations of the

uncontrolled model. Unfortunately, the changes of variables did not affect the convergence of the two algorithms.

5. Numerical simulations for Case I: low perceived relative risk of VSEs and relatively slow imitation

5.1 *General settings*

As mentioned in the previous section, we describe the case of low perceived relative risk of VSEs and relatively slow imitation by setting $\overline{\alpha} = 1/2000$ and $\overline{k} = 200$. Moreover, three positive values of seasonal amplitude are considered: $\sigma = 0.2$ (low seasonality), $\sigma = 0.5$ (moderate seasonality) and $\sigma = 0.9$ (large seasonality). The baseline case $\sigma = 0$ is also considered for the controlled case. The parameter values and initial data are reported in Tables 1 and 2.

5.2 *Case I: dynamics in absence of control*

When no control is implemented, the model predicts annual oscillations of both the disease burden and vaccine uptake (dash-dotted lines in Fig. 1). The fraction of vaccinated newborns, p, experiences immediate decline due to the onset of VSEs: from an initial value of 95% it falls below 10% in less than 1 year and then it starts to oscillate. In any case, the amplitude of oscillations grows gradually over the years until it reaches approximately a constant value. The time needed to 'converge' ranges between 4 years (when $\sigma = 0.9$) and 7 years (when $\sigma = 0.2$).

The prevalence peaks occur every year in April, after 2 months from the moment of maximum transmission rate. Instead, peaks of vaccine uptake occur only at the end of May, i.e. after about one season (3 months) from the moment of maximum transmission rate.

In Table 3 the extremal values of prevalence are reported, corresponding to different values of seasonal amplitude σ. As it can be seen, higher amplitudes of transmission rate are associated, not surprisingly, with higher peaks of disease prevalence. In particular, the maximum fraction of infective individual could increase about 90% as seasonality increases. Indeed, it increases from about 2.52×10^{-4} for $\sigma = 0.2$, up to 4.78×10^{-4} for $\sigma = 0.9$. Moreover, larger oscillations are associated with the larger value of seasonality (see again Table 3).

Since the perceived risk of infection is prevalence-dependent, also the maximum vaccination coverage increases from about 45% for $\sigma = 0.2$ up to 75% for $\sigma = 0.9$, respectively (right panels of Fig. 1).

TABLE 3 *Case I (low perceived relative risk of VSEs and relatively slow imitation): minimum and maximum values of prevalence in absence of control (I_m and I_M, resp.) and in presence of control (I_m^* and I_M^*, resp.) corresponding to different values of seasonal amplitude σ.*

σ	I_m	I_M	I_m^*	I_M^*
0.2	2.989×10^{-5}	2.519×10^{-4}	2.610×10^{-5}	5.651×10^{-5}
0.5	2.248×10^{-5}	3.787×10^{-4}	2.049×10^{-5}	7.388×10^{-5}
0.9	1.668×10^{-5}	4.782×10^{-4}	1.625×10^{-5}	1.011×10^{-4}

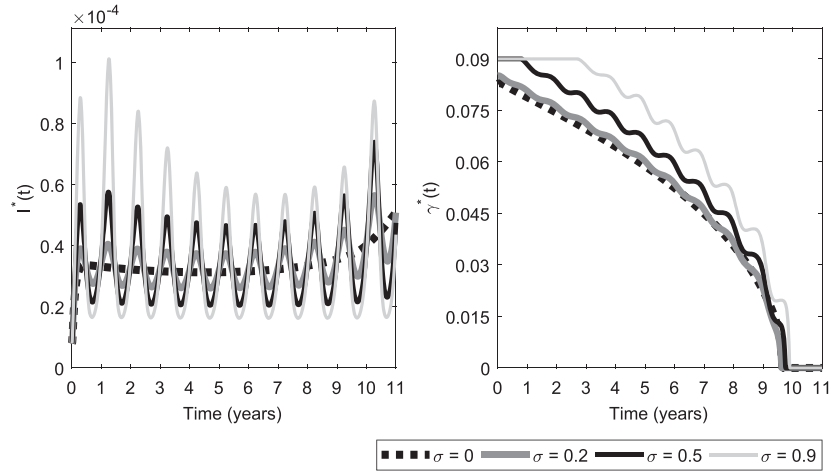

FIG. 2. Case I (low perceived relative risk of VSEs and relatively slow imitation): impact of the seasonality amplitude σ on the optimal fraction of infected individuals (left panel) and optimal control time profile (right panel) as predicted by model (2.5) with $\gamma(t)$ given by (3.3). Four values of seasonal amplitude are considered: $\sigma = 0$, $\sigma = 0.2$, $\sigma = 0.5$ and $\sigma = 0.9$. The other parameter values are reported in Tables 1 and 2.

5.3 *Case I: dynamics in presence of control*

If the PHS enacts public campaigns to favour vaccine uptake, higher efforts in supplying information are required as seasonality increases (see Fig. 2, right panel). In particular, when seasonality is large, the PHS efforts must be provided at their maximum level, $\gamma^*(t) = \gamma_{\max}(= 0.09)$ for almost 3 years. This period of maximum effort is reduced by 1 year when seasonality is moderate. Whereas, if seasonality is low, the optimal effort time profile $\gamma^*(t)$ begins at a value slightly below the maximum and slowly decreases towards the lower bound. In any case, optimal control is zero in the past 1–1.5 years of planning.

If PHIs are enacted according to the optimal time profile, the corresponding dynamics of p is initially larger than its uncontrolled time profile (see the solid lines in the right panels of Fig. 1). Moreover, the optimal vaccination coverage is characterized by small oscillations patterns. Once close to the time horizon, the vaccine coverage declines to such an extent that it becomes lower than it would have been in the uncontrolled case.

Note that a higher seasonality has beneficial effects on the vaccine uptake, as a consequence of the abovementioned fact that the PHS efforts increase with σ. Indeed, indicating with $t_x(\sigma) \geqslant 0$ the amplitude of the time interval $(0, t_x)$ during which p remains larger than a proportion x, given an amplitude σ, we have the following: i) $t_{0.8}(0.2) = 5.3$ years, whereas $t_{0.8}(0.9) \approx 7.3$ years; ii) $t_{0.4}(0.2) \approx 9.4$ years, whereas $t_{0.4}(0.9) \approx 9.9$ years (see Table 4).

The optimal intervention impacts the dynamics of infectious prevalence in two distinct ways (see Fig. 1, left panels): i) the annual average value of the prevalence is reduced w.r.t. the uncontrolled case; ii) the amplitude of the oscillations of the prevalence is strongly reduced w.r.t. the uncontrolled case. Note that although the seasonality strength positively impacts on the optimal vaccine uptake, we note that the prevalence increases with σ.

TABLE 4 *Case I (low perceived relative risk of VSEs and relatively slow imitation): time needed to reach the vaccination coverage* $p^* = 0.8$ *and* $p^* = 0.4$ *and total costs (given by (3.1)) corresponding to different values of seasonal amplitude* σ.

σ	$t_{0.8}(\sigma)$ (*years*)	$t_{0.4}(\sigma)$ (*years*)	Total costs (USD)
0	5.06	9.53	4.552×10^7
0.2	5.30	9.44	4.584×10^7
0.5	6.22	9.56	4.795×10^7
0.9	7.26	9.88	5.251×10^7

The total costs, i.e. the values of the objective functional (3.1) corresponding to the optimal time profile are reported in Table 4. The numerical simulations predict that costs will increase as seasonal amplitude increases and the difference can reach up to 15% approximately. Given the weights K_{in}, K_v and C_γ as in Table 2, the predicted cost of the whole PHIs campaign is approximately $\sim 5 \times 10^7$ USD.

6. Numerical simulations for Case II: intermediate perceived relative risk of VSEs and very slow imitation

6.1 *General settings*

We consider now the case of intermediate perceived relative risk of VSEs (represented by $\overline{\alpha} = 1/450$) and very slow imitation rate (represented by $\overline{k} = 5$). As in the previous case, we assume that three levels of seasonal amplitude (low, moderate and large) may be represented by $\sigma = 0.2$, $\sigma = 0.5$ and $\sigma = 0.9$, respectively. The baseline case $\sigma = 0$ is also considered for the controlled case. The parameter values and initial data are reported in Tables 1 and 2.

6.2 *Case II: dynamics in absence of control*

In the uncontrolled case ($\gamma(t) \equiv 0$), model (2.5) for Case II predicts an oscillating pattern of infectious individuals where amplitude increases along time and seems to approach a steady-state value (see dash-dotted lines in Fig. 3, left panels). Compared to Case I, the duration of the transient period to reach constant amplitudes is longer (from 7 to 8 years according to the strength of seasonality). The prevalence peaks (namely, I_M) are much higher than those observed in Case I (see Table 5 and compare with Table 3).

In Case II, the reduced imitation rate deeply impacts the pattern of vaccinated proportion. Indeed, in this case p decreases until it reaches a value close to 8–10% of the total population of parents after the first 3–4 years and then it exhibits minimal oscillations, whose amplitude is about 1% of the total population of parents (see dash-dotted lines in Fig. 3, right panels).

6.3 *Case II: dynamics in presence of control*

As illustrated in Fig. 4, right panel, a higher amplitude of seasonality requires greater efforts in enacting persuasive actions also for Case II. When the seasonality is large, $\sigma = 0.9$; the optimal public campaign effort $\gamma^*(t)$ is at its upper bound, $\gamma_{\max} = 0.01$, for about 2.5 years and then declines. When seasonality is moderate, $\sigma = 0.5$; the control starts at its upper bound and then rapidly decreases, while in the presence of low seasonality, $\sigma = 0.2$, the PHS effort must be initially provided at a value slightly less

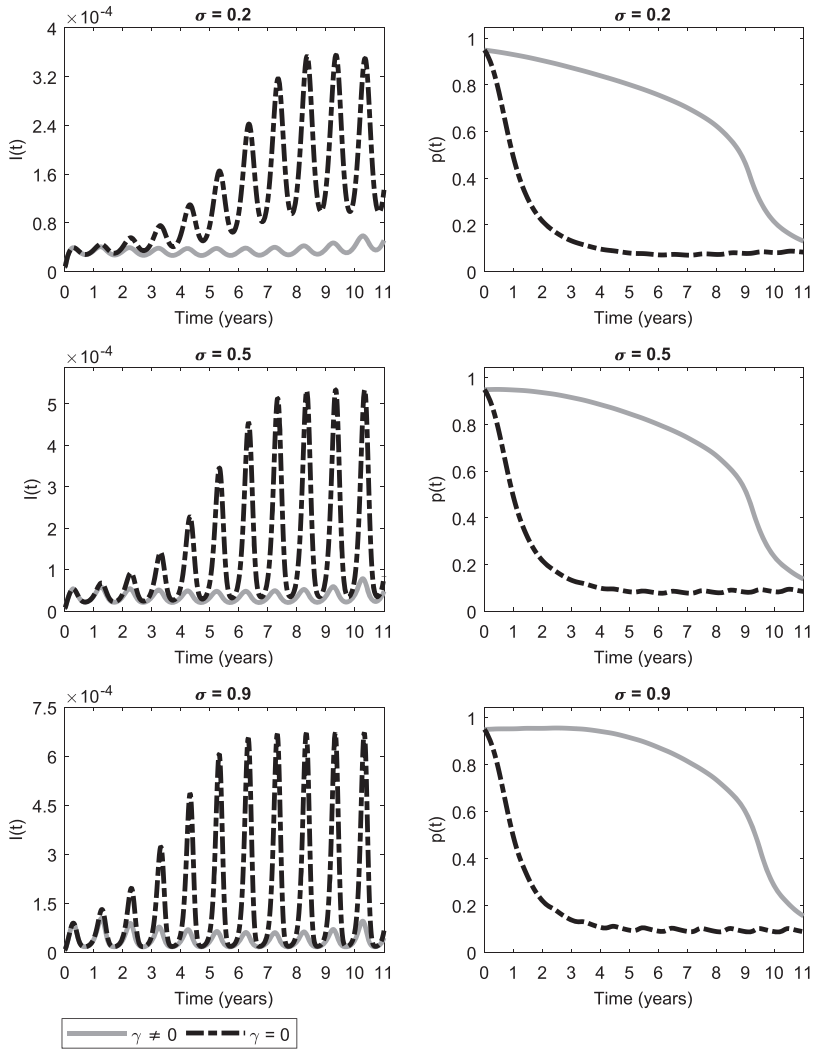

FIG. 3. Case II (intermediate perceived relative risk of VSEs and very slow imitation): impact of the seasonality amplitude σ on the dynamics of model (2.5). The dash-dotted (resp. solid) lines represent the time profiles in absence of control ($\gamma(t) \equiv 0$) (resp. with the optimal control given by (3.3)). Left panels: fraction of infectious individuals. Right panels: vaccinated proportion among newborns. First row: $\sigma = 0.2$, second row: $\sigma = 0.5$ and third row: $\sigma = 0.9$. The other parameter values are reported in Tables 1 and 2.

than $\gamma_{\max}$ before it starts to decline to zero. In each of these cases, no control strategies are enacted in the past 1.5–2 years of the planning horizon.

When optimal control is enacted the vaccine uptake is greatly affected. Indeed, p^* remains large for the vast majority of the time span (see the solid lines in the right panels of Fig. 3). Moreover, a higher seasonality has beneficial effects on the vaccine uptake. Indeed, we have the following: i) $t_{0.8}(0.2) \approx 5.0$ whereas $t_{0.8}(0.9) \approx 7.2$; and ii) $t_{0.4}(0.2) \approx 9.2$ whereas $t_{0.4}(0.9) = 9.6$ (see Table 6).

TABLE 5 *Case II (intermediate perceived relative risk of VSEs and very slow imitation): minimum and maximum values of prevalence in absence of control (I_m and I_M, resp.) and in presence of control (I_m^* and I_M^*, resp.) corresponding to different values of seasonal amplitude σ.*

σ	I_m	I_M	I_m^*	I_M^*
0.2	2.790×10^{-5}	3.535×10^{-4}	2.622×10^{-5}	5.850×10^{-5}
0.5	2.169×10^{-5}	5.317×10^{-4}	2.059×10^{-5}	7.808×10^{-5}
0.9	1.656×10^{-5}	6.699×10^{-4}	1.628×10^{-5}	1.036×10^{-4}

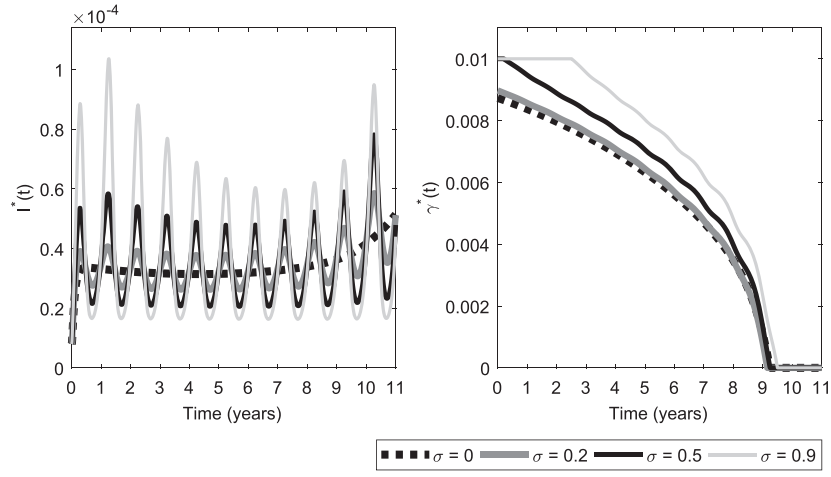

FIG. 4. Case II (intermediate perceived relative risk of VSEs and very slow imitation): impact of seasonality amplitude σ on the optimal fraction of infected individuals (left panel) and optimal control time profile (right panel) as predicted by model (2.5) (with $\gamma(t)$ given by (3.3)). Four values of seasonal amplitude are considered: $\sigma = 0, \sigma = 0.2, \sigma = 0.5$ and $\sigma = 0.9$. The other parameter values are reported in Tables 1 and 2.

TABLE 6 *Case II (intermediate perceived relative risk of VSEs and very slow imitation): time needed to reach the vaccination coverage $p^* = 0.8$ and $p^* = 0.4$ and total costs (given by (3.1)) corresponding to different values of seasonal amplitude σ.*

σ	$t_{0.8}(\sigma)$ (*years*)	$t_{0.4}(\sigma)$ (*years*)	Total costs (USD)
0	4.82	9.24	4.528×10^7
0.2	5.04	9.19	4.563×10^7
0.5	6.02	9.34	4.793×10^7
0.9	7.21	9.60	5.300×10^7

Although the vaccine uptake increases with σ, also here the reverse effect is observed on the prevalence: the higher is σ the larger are the oscillations of I^*. Of course, due to the low vaccine uptake in absence of control, the prevalence exhibits in all cases smaller oscillations and smaller annual average value than in the non-controlled case (left panels of Fig. 3).

In order to evaluate the interplay between seasonality and total expenditure by the PHS, the values assumed by the objective functional (3.1) are computed and reported in Table 6. As expected, higher amplitudes of seasonality are associated with higher costs. One can note that, although the order of magnitude of costs is the same with the corresponding values of Case I (compare Table 6 with Table 4), Case II results in about 5×10^5 USD saving compared to Case I for the same seasonality amplitude.

7. Impact of the latency rate on the model dynamics and the optimal control

The most characteristic parameter of a SEIR model is, of course, the latency rate (the parameter ρ in (2.5)). This rate is the inverse of the average latency period. When ρ is very large, the latency period is very small and the SEIR model behaves in practice as a SIR model. In this case an approximation can be obtained by means of the quasi steady state assumption

$$E \approx \frac{\beta(t)SI}{\mu + \rho},$$

leading to a slightly corrected contagion rate

$$CR = \frac{\rho}{\mu + \rho}\beta(t)SI.$$

Thus, it is of interest to assess the impact of the parameter ρ on the dynamics of the disease spread and the optimal control.
To this aim, we consider two values of latency rate, namely

$$\rho_1 = 0.2; \quad \rho_2 = 5\rho.$$

These values are sufficiently large and sufficiently small, without however being extremely low/large.

The most interesting effect is observed when the latency rate is ρ_1 (i.e. one-fifth of the baseline rate). Indeed, in such a case the presence of seasonality has a very small impact on the optimal control (Figs 5 and 6, third row) and on the corresponding vaccine propensity (Figs 5 and 6, second row as well as the left columns of Tables 7 and 8). If the latency rate is ρ_1 it can be also observed a reduction of the amplitude of the oscillations of the prevalence (Figs 5 and 6, first row). This was expected based on the following heuristic argument: the equation ruling the dynamics of E is equivalent to the model of a first-order linear low-pass filter (Chua *et al.*, 1987; Chen, 2009; Dimopoulos, 2011), whose input is the oscillating signal $\beta(t)SI$. Thus, by increasing the characteristic time of the filter (i.e. decreasing the latency rate) its filtering power increases due to the decrease of the cut-off frequency of the filter.

8. Conclusions

In this work we introduce a SEIR-like behaviour-dependent vaccination model, including seasonal fluctuations of the transmission rate and an awareness campaign by the PHS aimed at favouring the vaccine uptake by the target population.

Our aim is to find, via OCT, the optimal profile of the abovementioned PHS action to minimize the total costs of the disease. Two of the considered costs are customary in epidemiology: the vaccinations

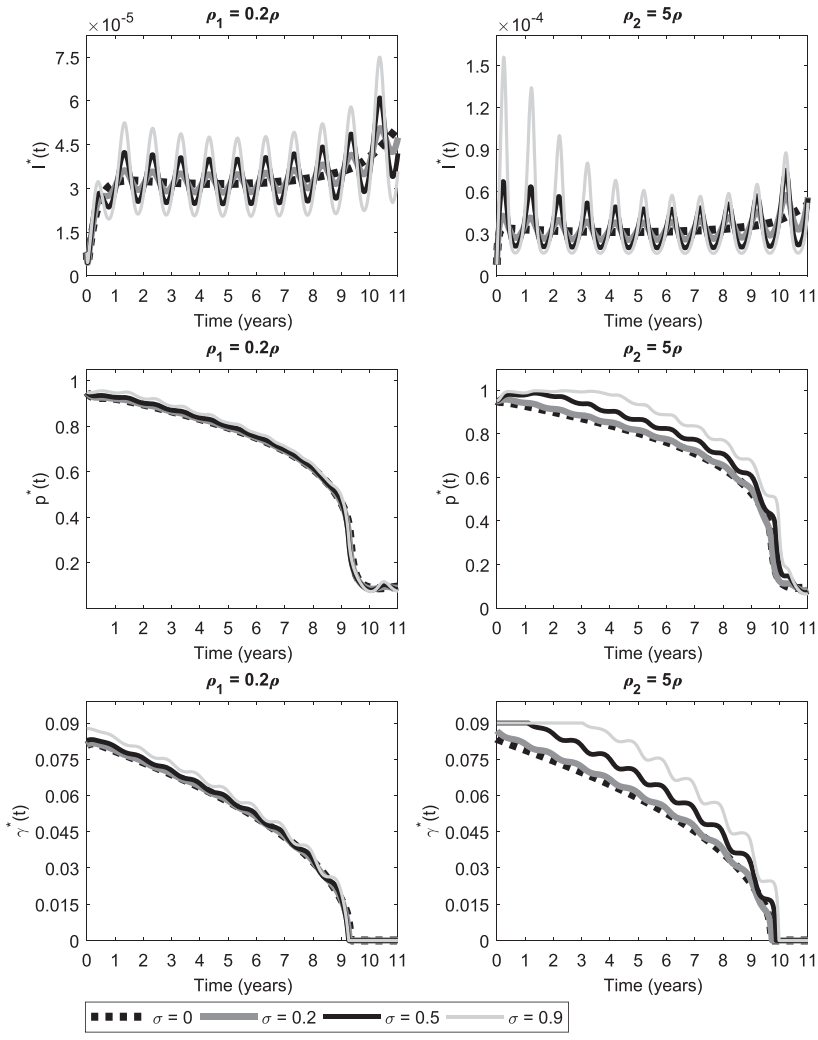

FIG. 5. Case I (low perceived relative risk of VSEs and relatively slow imitation): impact of the latency rate and of the seasonality amplitude on the dynamics of model (2.5) with $\gamma(t)$ given by (3.3). Left panels, latency rate: $\rho_1 = 0.2\rho$. Right panels, latency rate: $\rho_2 = 5\rho$. First row: dynamics of optimal fraction of infectious individuals, second row: optimal vaccinated proportion and third row: PHS efforts. Four values of seasonal amplitude σ are considered, as reported in the legend. Other parameter values are given in Tables 1 and 2.

costs (including the economic burden of vaccine-related side effects) and the costs related to the infections. However, here we also consider a third less usual category of costs (recently introduced in Buonomo *et al.*, n.d.), i.e. the economic burden to enact the PHS campaigns.

We apply the Pontryagin minimum principle to obtain the optimality conditions and numerically explore how three key epidemiologic 'dimensions' co-present in our control model impact on the control and spread of the target disease. These 'dimensions' are the seasonality, the human behaviour and the latency time/rate.

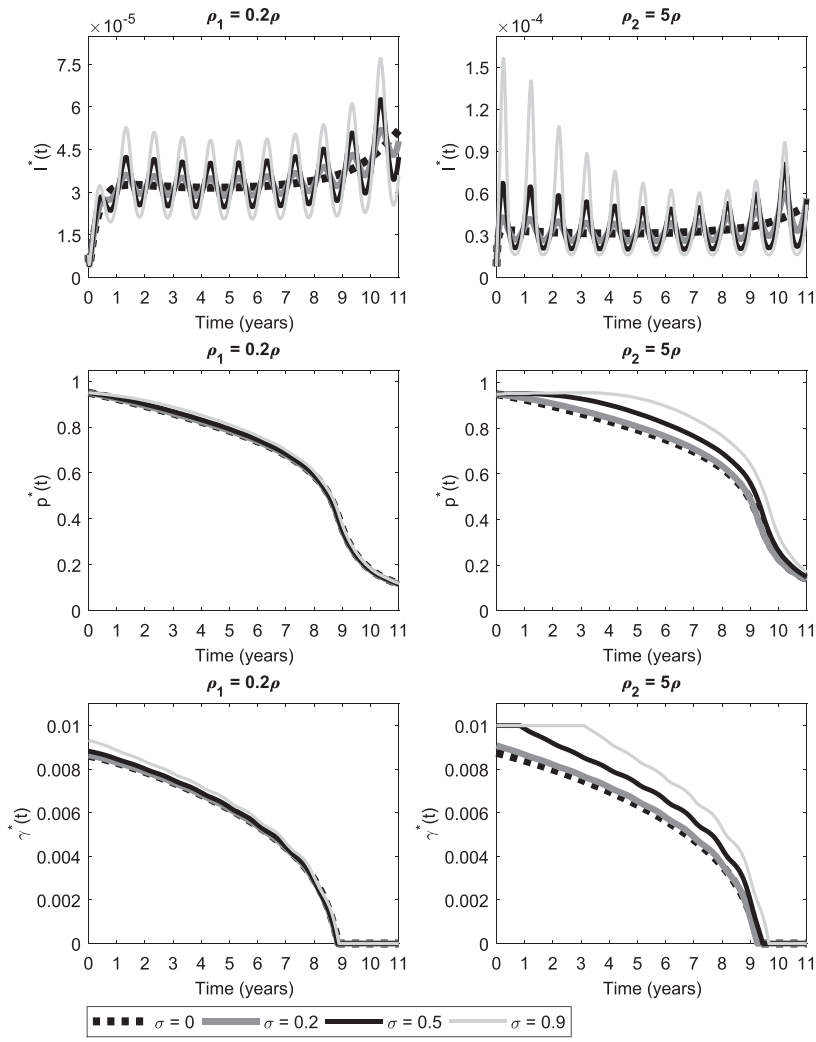

FIG. 6. Case II (intermediate perceived relative risk of VSEs and very slow imitation): impact of the latency rate and of the seasonality amplitude on the dynamics of model (2.5) with $\gamma(t)$ given by (3.3). Left panels, latency rate: $\rho_1 = 0.2\rho$. Right panels, latency rate: $\rho_2 = 5\rho$. First row: dynamics of optimal fraction of infectious individuals, second row: optimal vaccinated proportion and third row: PHS efforts. Four values of seasonal amplitude σ are considered, as reported in the legend. Other parameter values are given in Tables 1 and 2.

Due to its well-known impressive impact on disease time series and models (Altizer *et al.*, 2006; Grassly & Fraser, 2006; Buonomo *et al.*, 2018b), the seasonality degree is somewhat central in our analysis.

The human behaviour is summarized by the two parameters of the imitation game: the imitation speed and the perceived risk of VSEs compared to the perceived risk of infection. Namely, we considered two noteworthy case studies. In Case I (resp. Case II), the relative perceived risk of VSEs is low (resp. intermediate) and the speed of imitation is relatively low (resp. very low).

TABLE 7 *Case I (low perceived relative risk of VSEs and relatively slow imitation): impact of the latency rate and amplitude σ on the time needed to reach the vaccination coverage $p^* = 0.8$ and $p^* = 0.4$.*

	$\rho_1 = 0.2\rho$		$\rho_2 = 5\rho$	
σ	$t_{0.8}(\sigma)(years)$	$t_{0.4}(\sigma)(years)$	$t_{0.8}(\sigma)(years)$	$t_{0.4}(\sigma)(years)$
0	4.87	9.21	5.10	9.59
0.2	4.86	9.17	5.38	9.52
0.5	4.99	9.16	6.38	9.82
0.9	5.51	9.19	7.39	9.98

TABLE 8 *Case II (intermediate perceived relative risk of VSEs and very slow imitation): impact of the latency rate and amplitude σ on the time needed to reach the vaccination coverage $p^* = 0.8$ and $p^* = 0.4$.*

	$\rho_1 = 0.2\rho$		$\rho_2 = 5\rho$	
σ	$t_{0.8}(\sigma)(years)$	$t_{0.4}(\sigma)(years)$	$t_{0.8}(\sigma)(years)$	$t_{0.4}(\sigma)(years)$
0	4.61	8.88	4.86	9.32
0.2	4.63	8.86	5.19	9.28
0.5	4.80	8.87	6.40	9.50
0.9	5.21	8.94	7.61	9.79

In the first set of simulations we choose a baseline value for the latency rate and investigate the interplay between seasonality and behaviour. Then, based on these results, we assess how they could change in case of small or large latency time.

The ensuing analysis points out the following results:

- The degree of seasonality of the transmission rate produces a remarkable impact on the efforts needed by the PHS to enact an optimal control of the disease. Generally speaking, a higher amplitude of the seasonal variation produces a higher effort and, not surprisingly, higher costs. This increased level of efforts, in turn, beneficially impacts on the induced vaccine uptake since the larger is the strength of seasonality σ, the longer the vaccine propensity remains large. On the other hand, the increase in vaccine propensity is not mirrored by a decrease of the disease prevalence, which, on the contrary, increases with σ. Thus, we may say that although the seasonality-dependent increase of efforts produces an increase of vaccine uptake, such increase is not able (at least for the parametric set we explored in our simulations) to fully compensate the direct action of seasonality on the prevalence.
- Not surprisingly, we found that in all the analysed cases the prevalence induced by the optimal control is smaller and exhibits smaller oscillations compared to the uncontrolled dynamics.
- As far as the global effect of optimal control on the oscillations of both vaccine uptake and of disease prevalence is concerned, the optimal control seems to totally (for p) or partially (for I) suppress the observed oscillations.
- As far as the role of the parameters that tune the human behavioural response is concerned, comparing the Case I (low relative perceived risk of VSEs and relatively low imitation speed) with Case II (intermediate relative perceived risk of VSEs and very low imitation speed), we

found the following: i) in Case II the control is practically unaffected by the oscillations of $\beta(t)$ at variance with Case I where small oscillations are present especially in the second part of the control horizon; and ii) the control-induced dynamics of p are quite similar and in both cases are unaffected by oscillations.

- Finally, the impact of the latency time, which is the most characteristic parameter of the SEIR model, is particularly important when it is large (i.e. when the latency rate is low). Indeed, in such a case the effect of seasonality on the optimal control time profile and on the vaccine propensity p is negligible. Moreover, the amplitudes of the oscillations are reduced; this can be heuristically explained as a low-pass filtering effect of the buffer compartment E. Indeed, the differential equation for E is equivalent to the mathematical model of the classical first-order low-pass filter (Chua *et al.*, 1987; Chen, 2009; Dimopoulos, 2011).
- As far as the interplay between latency and behaviour is concerned, in the case of smaller latency time it is observed for Case II a reduced amount of oscillations w.r.t. the Case I, as we had observed for simulations corresponding to the baseline value of the latency time.

Although our results are preliminary and not yet supported by field data, the analysis proposed here represents a further step in using 'simple' mathematical models to identify the role of private and public communication in determining the observed vaccination coverage. In particular, the first of the above points can provide some suggestions of interest to PHSs planning vaccine awareness campaigns for diseases strongly impacted by seasonalities. Indeed, it shows that although the campaigns can deeply influence the vaccine uptake by the target population, the response in term of reduction of prevalence may appear not so amazing. This is simply an appearance caused by the strong nonlinearity of the disease dynamics, since the prevalence in absence of any awareness campaigns would be much larger. Another message is that the presence of seasonal oscillations in the transmission rate is not mirrored by wild oscillations of the control. The OC analysis showed that the efforts must be increased and do not follow the seasonal pattern. This is an interesting point, since one could naively think that the effort should be in phase and also in quantitative agreement with the changes of the contact rate (i.e. much more effort during the high contacts period, much less effort during the low contacts periods). On the contrary, we observed that, grossly, the control has small oscillations and they are—roughly speaking—in phase opposition to the contact rate.

Of course, more complex metapopulation models might provide more useful indications coming from emerging properties that are absent in simple models as the SEIR one.

As far as the numerical simulations are concerned, our priority will be finding a simulation tool that could allow us to fully explore a range of realistic initial conditions.

Finally, it is important to stress an important limitation of many works, including ours, applying OCT to infectious diseases. Namely, although our time horizon is usually relatively small with respect to large demographic changes, nevertheless, the assumption of constant death and birth rates is an idealization, as shown in (d'Onofrio *et al.*, 2008). In Appendix A, we investigated the effect of an exponential increase of the population, which yielded small deviations from the case of static population. However, in order to have a sufficiently realistic idea of the impact of human demography on the problem in study one should take into account not only deterministic 'internal' demographic trends (d'Onofrio *et al.*, 2008) but also their stochastic fluctuations that sometimes can induce relevant unexpected effects (Alonso *et al.*, 2007; Black & McKane, 2010). We are investigating the impact of these changes, which imply further layers of modelling complexity, among which are as follows: i) the inclusion of systematic and punctual immigration and emigration fluxes: ii) the correct modelling of the stochastic perturbation affecting the

system, e.g. by means of bounded stochastic processes (d'Onofrio, 2013): iii) the interplay between seasonality and demographic stochasticity (Black & McKane, 2010); and last but not least iv) the determination of the optimal control in the stochastic setting (Fleming & Rishel, 1975), since it would be of interest to assess the robustness of the optimal control with respect to the abovementioned heterogeneities.

Acknowledgements

The work of B.B. and R.D.M. has been performed under the auspices of the Italian National Group for the Mathematical Physics of the National Institute for Advanced Mathematics. We thank two anonymous referees for their precious suggestions that helped us to greatly improve this work.

References

Alonso, D., McKane, A. J. & Pascual, M. (2007) Stochastic amplification in epidemics. *J. R. Soc. Interface*, **4**, 575–582.

Altizer, S., Dobson, A., Hosseini, P., Hudson, P., Pascual, M. & Rohani, P. (2006) Seasonality and the dynamics of infectious diseases. *Ecol. Lett.*, **9**, 467–484.

Andre, F. E., Booy, R., Bock, H. L., Clemens, J., Datta, S. K., John, T. J., Lee, B. W., Lolekha, S., Peltola, H., Ruff, T., Santosham, M. & Schmitt, H. J. (2008) Vaccination greatly reduces disease, disability, death and inequity worldwide. *Bull. World Health Organ.*, **86**, 140–146.

Aniţa, S. & Capasso, V. (2012) Stabilization of a reaction–diffusion system modelling a class of spatially structured epidemic systems via feedback control. *Nonlinear Anal. Real World Appl.,* **13**, 725–735.

Aniţa, S., Capasso, V. & Arnăutu, V. (2011) *An Introduction to Optimal Control Problems in Life Sciences and Economics*. New York: Birkhäuser/Springer.

Arnăutu, V., Barbu, V. & Capasso, V. (1989) Controlling the spread of a class of epidemics. *Appl. Math. Optim.*, **20**, 297–317.

Bauch, C. T. (2005) Imitation dynamics predict vaccinating behaviour. *Proc. R. Soc. Lond. B Biol. Sci.*, **272**, 1669–1675.

Black, A. J. & McKane, A. J. (2010) Stochastic amplification in an epidemic model with seasonal forcing. *J. Theor. Biol.*, **267**, 85–94.

Blayneh, K. W., Gumel, A. B., Lenhart, S. & Clayton, T. (2010) Backward bifurcation and optimal control in transmission dynamics of West Nile virus. *Bull. Math. Biol.*, **72**, 1006–1028.

Buonomo, B., Carbone, G. & d'Onofrio, A. (2018a) Effect of seasonality on the dynamics of an imitation-based vaccination model with public health intervention. *Math. Biosci. Eng.*, **15**, 299–321.

Buonomo, B., Chitnis, N. & d'Onofrio, A. (2018b) Seasonality in epidemic models: a literature review. *Ric. Mat*., **67**, 7–25.

Buonomo, B., d'Onofrio, A. & Lacitignola, D. (2013) Modeling of pseudo-rational exemption to vaccination for SEIR diseases. *J. Math. Anal. Appl.*, **404**, 385–398.

Buonomo, B., d'Onofrio, A. & Manfredi, P. (n.d.) Public health intervention to shape voluntary vaccination: continuous and piecewise optimal control. (Submitted).

Capasso, V. (1993) *Mathematical Structures of Epidemic Systems*. Berlin: Springer.

Capasso, V. & Serio, G. (1978) A generalization of the Kermack–McKendrick deterministic epidemic model. *Math. Biosci.*, **42**, 43–61.

Carabin, H., Edmunds, W. J., Kou, U., Van den Hof, S. & Van Hung, N. (2002) The average cost of measles cases and adverse events following vaccination in industrialised countries. *BMC Public Health*, **2**, 22.

Casiday, R., Cresswell, T., Wilson, D. & Panter-Brick, C. (2006) A survey of UK parental attitudes to the MMR vaccine and trust in medical authority. *Vaccine*, **24**, 177–184.

Centers for Disease Control and Prevention (2017) *Protect your baby with immunization*. https://www.cdc.gov/features/infantimmunization/. (Accessed on December 2017).

Chen, W.-K. (ed.) (2009) *Fundamentals of Circuits and Filters*. Boca Raton: CRC Press.

Chua, L. O., Desoer, C. A. & Kuh, E. S. (1987) *Linear and Nonlinear Circuits*. New York: McGraw-Hill.

De la Sen, M., Ibeas, A. & Alonso-Quesada, S. (2012) On vaccination controls for the SEIR epidemic model. *Commun. Nonlinear Sci. Numer. Simul.*, **17**, 2637–2658.

Dimopoulos, H. G. (2011) *Analog Electronic Filters: Theory, Design and Synthesis*. Dordrecht, London: Springer.

d'Onofrio, A. (2002) Stability properties of pulse vaccination strategy in SEIR epidemic model. *Math. Biosci.*, **179**, 57–72.

d'Onofrio, A. (ed.) (2013) *Bounded Noises in Physics, Biology, and Engineering*. New York: Birkhäuser/ Springer.

d'Onofrio, A., Manfredi, P. & Poletti, P. (2011) The impact of vaccine side effects on the natural history of immunization programmes: an imitation-game approach. *J. Theor. Biol.*, **273**, 63–71.

d'Onofrio, A., Manfredi, P. & Poletti, P. (2012) The interplay of public intervention and private choices in determining the outcome of vaccination programmes. *PLoS One*, **7**, e45653.

d'Onofrio, A., Manfredi, P. & Salinelli, E. (2008) Fatal SIR diseases and rational exemption to vaccination. *Math. Med. Biol.*, **25**, 337–357.

Dubé, E., Laberge, C., Guay, M., Bramadat, P., Roy, R. & Bettinger, J. A. (2013) Vaccine hesitancy: an overview. *Hum. Vaccin. Immunother.*, **9**, 1763–1773.

Earn, D. J., Rohani, P., Bolker, B. M. & Grenfell, B. T. (2000) A simple model for complex dynamical transitions in epidemics. *Science*, **287**, 667–670.

Fleming, W. H. & Rishel, R. W. (1975) *Deterministic and Stochastic Optimal Control. Applications of Mathematics*, vol. **1**. New York: Springer.

Fu, F., Rosenbloom, D. I., Wang, L. & Nowak, M. A. (2011) Imitation dynamics of vaccination behaviour on social networks. *Proc. R. Soc. Lond. B Biol. Sci.*, **278**, 42–49.

Grass, D., Caulkins, J. P., Feichtinger, G., Tragler, G. & Behrens, D. A. (2008) *Optimal Control of Nonlinear Processes*. Berlin: Springer.

Grassly, N. C. & Fraser, C. (2006) Seasonal infectious disease epidemiology. *Proc. R. Soc. Lond. B Biol. Sci.*, **273**, 2541–2550.

Gromov, D., Bulla, I., Romero-Severson, E. O. & Serea, O. S. (2017) Numerical optimal control for HIV prevention with dynamic budget allocation. *Math. Med. Biol.*(in press).

Institut National de la Statistique et des Études Économiques. (2018) *Bilan démographique 2017*. https://www.insee.fr/fr/statistiques/1892117?sommaire=1912926. (In French) (Accessed on April 2018).

Istituto Superiore di Sanità. (2017) *Obbligo vaccinale: cos'è e perché è importante*. http://www.epicentro.iss.it/temi/vaccinazioni/ObbligoVaccinale.asp. (In Italian) (Accessed on November 2017).

Jansen, V. A., Stollenwerk, N., Jensen, H. J., Ramsay, M., Edmunds, W. & Rhodes, C. (2003) Measles outbreaks in a population with declining vaccine uptake. *Science*, **301**, 804.

Laguzet, L. & Turinici, G. (2015) Global optimal vaccination in the SIR model: properties of the value function and application to cost-effectiveness analysis. *Math. Biosci.*, **263**, 180–197.

Ledzewicz, U., Aghaee, M. & Schättler, H. (2016) Optimal control for a SIR epidemiological model with time-varying populations. *2016 IEEE Conference on Control Applications (CCA).* Buenos Aires: IEEE, pp. 1268–1273.

Ledzewicz, U. & Schättler, H. (2011) On optimal singular controls for a general SIR-model with vaccination and treatment. *Discrete Contin. Dyn. Syst.*, Supplement 2011, 981–990.

Lee, S., Chowell, G. & Castillo-Chávez, C. (2010) Optimal control for pandemic influenza: the role of limited antiviral treatment and isolation. *J. Theor. Biol.*, **265**, 136–150.

Lenhart, S. & Workman, J. T. (2007) *Optimal Control Applied to Biological Models*. London: CRC Press.

Livi-Bacci, M. (2017) *A Concise History of World Population*, 6th edn. Chichester: Wiley–Blackwell.

Manfredi, P. & d'Onofrio, A. (eds) (2013) *Modeling the Interplay Between Human Behavior and the Spread of Infectious Diseases*. New York: Springer.

Mbah, M. L. N., Liu, J., Bauch, C. T., Tekel, Y. I., Medlock, J., Meyers, L. A. & Galvani, A. P. (2012) The impact of imitation on vaccination behavior in social contact networks. *PLoS Comput. Biol.*, **8**, e1002469.

Metcalf, C., Ferrari, M., Graham, A. & Grenfell, B. (2015) Understanding herd immunity. *Trends Immunol.*, **36**, 753–755.

Ministère des Solidarités et de la Santé. (2017) 11 vaccins obligatoires en 2018. http://solidarites-sante.gouv.fr/prevention-en-sante/preserver-sa-sante/vaccination/vaccins-obligatoires/article/11-vaccins-obligatoires-en-2018-le-projet-de-loi. (In French) (Accessed on December 2017).

Mwanga, G. G., Haario, H. & Capasso, V. (2015) Optimal control problems of epidemic systems with parameter uncertainties: application to a malaria two-age-classes transmission model with asymptomatic carriers. *Math. Biosci.*, **261**, 1–12.

Ndeffo Mbah, M. L. & Gilligan, C. A. (2013) Optimal control of disease infestations on a lattice. *Math. Med. Biol.*, **31**, 87–97.

NSW Ministry of Health. (2014) Infectious diseases of childhood fact sheet. http://www.health.nsw.gov.au/Infectious/factsheets/Pages/childhood.aspx. (Accessed on November 2017).

Omer, S. B., Salmon, D. A., Orenstein, W. A., Dehart, M. P. & Halsey, N. (2009) Vaccine refusal, mandatory immunization, and the risks of vaccine–preventable diseases. *N. Engl. J. Med.*, **360**, 1981–1988.

Perisic, A. & Bauch, C. T. (2009) Social contact networks and disease eradicability under voluntary vaccination. *PLoS Comput. Biol.*, **5**, e1000280.

Pontryagin, L., Boltyanskii, V., Gamkrelidze, R. & Mishenko, E. (1962) *The Mathematical Theory of Optimal Processes*. New York: Wiley Interscience. (Translated from the Russian by Trigoroff, K. N.).

Prosper, O., Ruktanonchai, N. & Martcheva, M. (2014) Optimal vaccination and bednet maintenance for the control of malaria in a region with naturally acquired immunity. *J. Theor. Biol.*, **353**, 142–156.

Public Health Wales Protection Division. (2013) *Actions supporting MMR vaccine uptake in children in Wales*. http://www.wales.nhs.uk/sitesplus/888/page/66797. (Accessed on November 2017).

Public Health Wales Protection Division. (2017) *National immunisation uptake data*. http://www.wales.nhs.uk/sites3/page.cfm?orgid=457&pid=54144. (Accessed on December 2017).

Reluga, T. C. & Galvani, A. P. (2011) A general approach for population games with application to vaccination. *Math. Biosci.*, **230**, 67–78.

Rodrigues, H. S., Monteiro, M. T. T. & Torres, D. F. (2014) Vaccination models and optimal control strategies to dengue. *Math. Biosci.*, **247**, 1–12.

Salvarani, F. & Turinici, G. (2018) Optimal individual strategies for influenza vaccines with imperfect efficacy and durability of protection. *Math. Biosci. Eng.*, **15**, 629–652.

Screening & Immunisations Team, NHS Digital. (2016) NHS immunisations statistics: England 2015–16, national statistics. http://digital.nhs.uk/catalogue/PUB21651.

Sharomi, O. & Malik, T. (2017) Optimal control in epidemiology. *Ann. Oper. Res.*, **251**, 55–71.

Shim, E., Kochin, B. & Galvani, A. (2009) Insights from epidemiological game theory into gender-specific vaccination against rubella. *Math. Biosci. Eng.*, **6**, 839–854.

Sobo, E. J. (2016) What is herd immunity, and how does it relate to pediatric vaccination uptake? US parent perspectives. *Soc. Sci. Med.*, **165**, 187–195.

Sun, C. & Hsieh, Y.-H. (2010) Global analysis of an SEIR model with varying population size and vaccination. *Appl. Math. Model.*, **34**, 2685–2697.

Wang, Z., Bauch, C. T., Bhattacharyya, S., d'Onofrio, A., Manfredi, P., Perc, M., Perra, N., Salathé, M. & Zhao, D. (2016) Statistical physics of vaccination. *Phys. Rep.*, **664**, 1–113.

World Health Organization. (2017) *Measles*. Fact sheet. http://www.who.int/mediacentre/factsheets/fs286/en/. (Accessed on December 2017).

Appendix A. Effects of idealized demographic changes

Our analysis was done under the hypothesis of constant population. However, many countries experience an appreciable demographic dynamics with a trend of population increase (Livi-Bacci, 2017;

Institut National de la Statistique et des Études Économiques, 2018). Modelling such increase, often characterized by an interplay of deterministic trends and stochastic fluctuations, is beyond the aim of this work and will be analysed in the future. However, given a simple demographic deterministic model, it can be of interest to assess which is its implication on the results we illustrated in the previous sections.

As a consequence, let us assume that the population size is exponentially increasing as result of the unbalance between a constant death rate μ and a larger constant birth rate $b > \mu$. Denoting as Z the population size at time t and continuing to denote as N its initial value (i.e. at $t = 0$), it yields

$$Z = e^{at}N,$$

where $a = b - \mu$.

Since the time horizon we have adopted is relatively short with respect to demographic characteristic times, this can be considered a satisfactory approximation, under the further hypothesis of lack of substantial unbalance between migratory inflow and outflow. We stress that the latter is another strong idealization of the current worldwide scenarios, but it is very good when examining past scenarios.

In such a case let us denote by X, U, Y, W the total number of susceptible, latent, infectious and removed individuals at time t, respectively. Assuming as in d'Onofrio *et al.* (2008) a realistic contagion rate of the type $\beta(t)(Y/Z)X$ (see in Wang *et al.*, 2016 a stochastic justification of why this contagion rate is preferable to the pure mass action version) yields the following:

$$\begin{aligned}
\dot{X} &= bZ - bZp - \mu X - \beta(t)\frac{Y}{Z}X \\
\dot{U} &= \beta(t)\frac{Y}{Z}X - (\mu + \rho)\, U \\
\dot{Y} &= \rho U - (\mu + \nu)\, Y \\
\dot{W} &= \nu Y - \mu W.
\end{aligned}$$

Passing to the epidemic fractions

$$(S, E, I, R) = \frac{1}{Z}(X, U, Y, W)$$

and taking into account that $\dot{Z} = (b - \mu)Z$ one easily gets

$$\begin{aligned}
\dot{S} &= b(1 - p) - bS - \beta(t)SI \\
\dot{E} &= \beta(t)SI - (b + \rho)\, E \\
\dot{I} &= \rho E - (b + \nu)\, I \\
\dot{R} &= \nu I - bR.
\end{aligned} \tag{A.1}$$

As far as the imitation game is concerned, it can be shown that the equation for p is unchanged. Indeed, indicating with P the total number of pro-vaccine subjects at time t, its dynamics is ruled by

$$\dot{P} = -k_0\alpha\frac{P}{Z}\frac{Z - P}{Z}P + k_0\theta I\frac{P}{Z}(Z - P) + \gamma(t)(Z - P) + aP$$

and from $p = P/Z$ one gets again (2.4).
As far as the costs are concerned, since the population is no more constant it follows that

$$J_{in} = \int_0^{t_f} e^{-rt} K_{in} N e^{at} \rho E \, \mathrm{d}t,$$
$$J_v = \int_0^{t_f} e^{-rt} K_v N e^{at} bp \, \mathrm{d}t,$$
$$J_\gamma = \int_0^{t_f} e^{-rt} C_\gamma e^{at} \gamma^2(t) \, \mathrm{d}t.$$

As a consequence the full objective functional now reads as follows:

$$J(\gamma(t)) = J_{in} + J_v + J_\gamma = \int_0^{t_f} e^{-r_{new} t} \left[C_\varphi E + C_v p + C_\gamma \gamma^2(t) \right] \mathrm{d}t, \tag{A.2}$$

where

$$r_{new} = r - a$$

and $C_\varphi = K_{in} N \rho$, $C_v = K_v N b$.

The adjoint system is the following:

$$\dot{\lambda_1} = r_{new}\lambda_1 + (\lambda_1 - \lambda_2)\,\beta_{avg}\left[1 + \sigma\cos(\omega t + \chi)\right] I + b\lambda_1$$
$$\dot{\lambda_2} = r_{new}\lambda_2 - C_\varphi + \rho(\lambda_2 - \lambda_3) + b\lambda_2$$
$$\dot{\lambda_3} = r_{new}\lambda_3 + (\lambda_1 - \lambda_2)\,\beta_{avg}\left[1 + \sigma\cos(\omega t + \chi)\right] S + \lambda_3(b + \nu) - \nu\lambda_4 - k_0\theta\lambda_5\left(p - p^2\right)$$
$$\dot{\lambda_4} = r_{new}\lambda_4 + b\lambda_4$$
$$\dot{\lambda_5} = r_{new}\lambda_5 - C_v + b\lambda_1 + \lambda_5\left[k_0(-3\alpha p^2 + 2\alpha p + 2\theta I p - \theta I) + \gamma(t)\right].$$

As far as the numerical values of μ, ν, $\beta(t)$ and of the initial conditions are concerned, we used the same values used in the main text. As far as b is concerned, we made the choice to adopt a birth rate such that the ratio b/μ was sufficiently realistic. Thus, we adopted as reference data those published by the National Statistical Institute of France (Institut National de la Statistique et des Études Économiques, 2018), a nation that in the past four decades is experiencing a steady births–deaths unbalance (Institut National de la Statistique et des Études Économiques, 2018). Under the exponential growth hypothesis, the ratio between the yearly number of births B over the yearly number of deaths D reads as follows:

$$\frac{B}{D} = \frac{\int_t^{t+1\text{ year}} bZ \, \mathrm{d}\tau}{\int_t^{t+1\text{ year}} \mu Z \, \mathrm{d}\tau} = \frac{b}{\mu}.$$

For France, the mean of B/D between 1999 and 2014 is about 1.46, so we set $b = 1.46\mu$, implying $a = 0.46\mu$.
Our simulations for both Cases I (see Fig. A1) and II (not shown) show that the impact of the considered deterministic demographic trends is small. For $\sigma \in \{0.5, 0.8\}$ (see the two lower panels of Fig. A1), the impact, initially null, is increasing towards the end, where due to the smallness of the control it can become relatively important. In the cases $\sigma \in \{0, 0.2\}$ (see the two upper panels of Fig. A1), instead, we observed since the start of the time horizon a small but systematic increase of the values of the control function with respect to the control obtained in the case of constant population. For $\sigma = 0$, this

is mirrored by a systematic increase of the prevalence, which is about 20% higher at t_f w.r.t. the case of constant population.

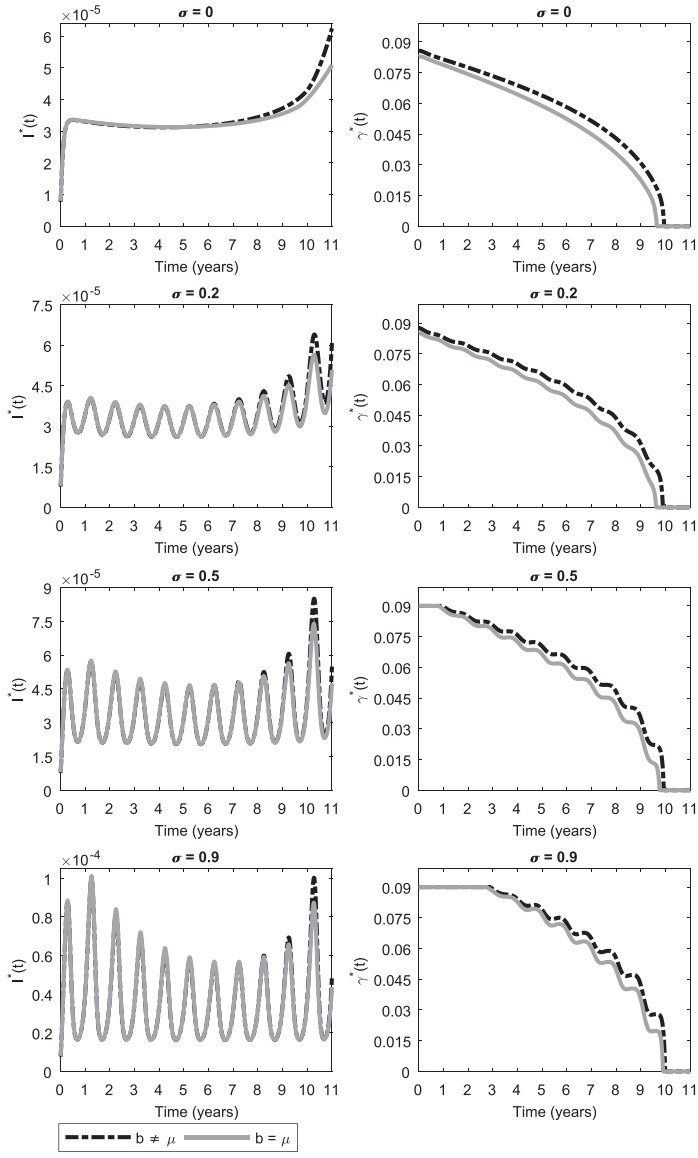

FIG. A1. Impact of an exponential growth of the population versus the case of constant population. The population size Z is $Z = Ne^{at}$, where $a = b - \mu$ and $b = 1.46\mu$ (exponential growth) or $b = \mu$ (constant population). Case I (low perceived relative risk of VSEs and relatively slow imitation): optimal fraction of infected individuals (left panels) and optimal control time profile (right panels). The dash-dotted (resp. solid) lines refer to the case $b = 1.46\mu$ (resp. $b = \mu$). Four values of seasonal amplitude are considered: $\sigma = 0$ (first row), $\sigma = 0.2$ (second row), $\sigma = 0.5$ (third row) and $\sigma = 0.9$ (fourth row). The other parameter values are reported in Table 1 and Table 2 or indicated in the text.